PHYSICAL REVIEW D **78,** 044031 (2008)

# Blandford's argument: The strongest continuous gravitational wave signal

Benjamin Knispel* and Bruce Allen+

*Max-Planck-Institut für Gravitationsphysik (Albert-Einstein-Institut) and Leibniz Universität Hannover Callinstr. 38, 30167 Hannover, Germany*

(Received 28 April 2008; published 14 August 2008)

For a uniform population of neutron stars whose spin-down is dominated by the emission of gravitational radiation, an old argument of Blandford states that the expected gravitational-wave amplitude of the nearest source is independent of the deformation and rotation frequency of the objects. Recent work has improved and extended this argument to set upper limits on the expected amplitude from neutron stars that *also* emit electromagnetic radiation. We restate these arguments in a more general framework, and simulate the evolution of such a population of stars in the gravitational potential of our galaxy. The simulations allow us to test the assumptions of Blandford's argument on a realistic model of our galaxy. We show that the two key assumptions of the argument (two dimensionality of the spatial distribution and a steady-state frequency distribution) are in general not fulfilled. The effective scaling dimension $D$ of the spatial distribution of neutron stars is significantly larger than two, and for frequencies detectable by terrestrial instruments the frequency distribution is not in a steady state unless the ellipticity is unrealistically large. Thus, in the cases of most interest, the maximum expected gravitational-wave amplitude *does* have a strong dependence on the deformation and rotation frequency of the population. The results strengthen the previous upper limits on the expected gravitational-wave amplitude from neutron stars by a factor of 6 for realistic values of ellipticity.

DOI: 10.1103/PhysRevD.78.044031 PACS numbers: 04.30.Db, 95.55.Ym, 97.60.Gb, 97.60.Jd

## I. INTRODUCTION

Continuous emission from spinning neutron stars is a promising source of gravitational waves, but so far no detections have been reported. This begs the question ''what is the largest expected amplitude of the continuous signal from nonaxisymmetric neutron stars?'' There might exist a (so far undetected) population of spinning neutron stars whose dominant energy loss goes into the production of gravitational waves, rather than into electromagnetic radiation. These are often called ''gravitars''; we show later in this paper that gravitars set an upper limit on the amplitude of gravitational waves from spinning neutron stars that are also emitting electromagnetic radiation.

In 1984, Blandford found a simple analytic relationship between the expected maximum amplitude of gravitational waves emitted by gravitars and their average galactic birthrate. This argument was not published, but it is documented by a citation in [1]. The argument was recently revised in [2]. This paper revises both the original and the revised Blandford arguments, and shows that two key assumptions of these arguments do not hold in a realistic galactic model of gravitars. This paper corrects the assumptions of the argument, and then investigates how the conclusions are affected by this change.

We stress that while this paper studies the behavior of a population of galactic gravitars, it does not make a plausibility case for the possible existence of such objects, or study their potential astrophysical implications. The study itself is nevertheless interesting, because even if gravitars do *not* exist, they provide a relevant upper bound on the gravitational-wave emission by objects (such as rapidly spinning neutron stars) that *do* exist.

The paper is organized as follows. Section II reviews Blandford's argument and its assumptions. A simple analytic calculation is used to derive the frequency-space distribution of the sources. This allows a sharper statement of the conclusion and clarifies the dependence upon the assumptions. The aim of this paper is to test whether these assumptions are fulfilled in a realistic model of our galaxy and, if the assumptions do not hold, what the consequences are. Section III describes a numerical simulation of the Galaxy, and Sec. IV presents results for the simulated spatial and frequency distribution of gravitars at the present time. The simulated spatial distributions do not satisfy the assumptions of Blandford's argument: they are not two dimensional and uniform. Section V uses these simulated distributions to recompute the expected maximum gravitational-wave amplitudes from gravitars. As shown in [2], the maximum expected gravitational-wave amplitudes from gravitars are upper limits for the gravitational-wave amplitudes from neutron stars spinning down through combined electromagnetic and gravitational-wave emission. Previous work assumed that all neutron stars are formed with the same (high) birth frequency. Here, the argument is generalized to cover a continuous distribution of initial frequencies. This is followed by a short conclusion.

For realistic models of neutron stars, the general upper limit on gravitational-wave emission set by considering the gravitar case applies for gravitational-wave frequencies

*Benjamin.Knispel@aei.mpg.de
+Bruce.Allen@aei.mpg.de

 

$f \gtrsim 250$ Hz. The reader who wants to skip all the details and just see the final result is advised to look at Fig. 5, which is the main result of the paper.

## II. BLANDFORD'S ARGUMENT: AN ANALYTIC DESCRIPTION

### A. Frequency evolution and a first analysis

If a rotating neutron star has a nonaxisymmetric shape, it will radiate away rotational energy by the emission of gravitational waves. It is straightforward to derive the equations describing the frequency evolution of gravitars. Their spin-down due to their nonaxisymmetric shape is given by

$$\dot{f} = -\frac{32\pi^4}{5}\frac{GI}{c^5}\varepsilon^2 f^5, \tag{2.1}$$

where $f$ is the frequency of the emitted gravitational waves, which is twice the spin frequency of the gravitar. $G$ is Newton's gravitational constant, $I$ is the momentum of inertia with respect to the rotational axis, $c$ is the speed of light, and $\varepsilon = \frac{I_1 - I_2}{I}$ is the ellipticity of the gravitar. Integrating (2.1) gives the frequency of gravitational waves emitted at time $t$ as

$$f(t) = (f_{\mathrm{B}}^{-4} + \beta^{-1}\varepsilon^2 t)^{-1/4} \quad \text{with} \quad \beta = \frac{5}{128\pi^4}\frac{c^5}{GI}, \tag{2.2}$$

assuming an initial (birth) gravitational-wave frequency $f_{\mathrm{B}} = f(0)$. The constant $\beta$ is approximately

$$\beta^{1/3} = 5.3 \times \left(\frac{10^{38}\ \mathrm{kg\,m^2}}{I}\right)^{1/3}\ \mathrm{kHz}. \tag{2.3}$$

We infer from (2.2) the spin-down timescale

$$\tau_{\mathrm{GW}}(\varepsilon, f) := \beta\varepsilon^{-2}f^{-4} \approx 4.6\ \mathrm{Gyr}\left(\frac{10^{-7}}{\varepsilon}\right)^2\left(\frac{100\ \mathrm{Hz}}{f}\right)^4, \tag{2.4}$$

which is the time for a gravitar born at a gravitational-wave frequency $f_{\mathrm{B}} \gg f$ with ellipticity $\varepsilon$ to spin down to gravitational-wave frequency $f$ via the emission of gravitational waves. These equations allow one to calculate the gravitational-wave frequency at the present time for any gravitar given its birth frequency, ellipticity, and age. This in turn allows one to determine the frequency distribution of a population of gravitars.

The strain amplitude $h$ of gravitational waves emitted by a gravitar at distance $r$ to the detector and assuming optimal mutual orientation (gravitar sky position given by the unit vector orthogonal to the plane of the detector arms; gravitar spin axis parallel to this vector) is given by

$$h = 4\pi^2\frac{GI}{c^4}\frac{\varepsilon f^2}{r}. \tag{2.5}$$

Given a model for the spatial distribution of gravitars, this allows one to determine the distribution of gravitational-wave amplitudes.

Let us begin by giving Blandford's original argument in a more complete form than the single-paragraph version given in [1].

Assume there is a population of galactic gravitars, which remain undetected because they do not emit electromagnetic waves. Reference [3] (particularly Sec. 6 and the appendix) shows the conditions necessary for a neutron star to be a gravitar. Reference [4] is a simulation of a population of isolated neutron stars accreting matter from the interstellar medium and demonstrates that quite a few neutron stars may in fact meet these conditions. Taken together, these two papers establish a detailed plausibility argument for the possible existence of a population of gravitars.

Assume the neutron stars are uniformly distributed in a thin two-dimensional galactic disk with radius $R$ and assume that the time between gravitar births in our galaxy is constant: $\tau_{\mathrm{B}} \approx 30$ yrs. Assume that all gravitars are born with the same ellipticity $\varepsilon$ and high birth frequency $f_{\mathrm{B}}$. The frequency of each gravitar will then evolve according to (2.2).

Consider an interval $[f_1, f_2]$ of gravitational-wave frequencies with $f_1, f_2 \ll f_{\mathrm{B}}$. Let us consider wide ranges of frequencies corresponding to the broadband sensitivity of modern interferometric detectors. Then, from (2.2) the time a gravitar will spend in this interval of frequencies is

$$t_{12} = \left[1 - \left(\frac{f_1}{f_2}\right)^4\right]\tau_{\mathrm{GW}}(\varepsilon, f_1). \tag{2.6}$$

The number of sources in this frequency interval is given by $N_{12} = \frac{t_{12}}{\tau_{\mathrm{B}}}$ if $t_{12} \geq \tau_{\mathrm{B}}$ and depends on the choice of the frequency band. Because of the assumed two dimensionality and uniformity of the spatial distribution the average distance $r_{\mathrm{cl}}$ to the closest gravitar in this range of frequencies can be written as

$$r_{\mathrm{cl}} = \frac{R}{\sqrt{N_{12}}} = R\sqrt{\frac{\tau_{\mathrm{B}}}{\tau_{\mathrm{GW}}(\varepsilon, f_1)}}\left[1 - \left(\frac{f_1}{f_2}\right)^4\right]^{-1/2}. \tag{2.7}$$

The formula given in Ref. [1] agrees with Eq. (2.7), if one assumes that the factor in square brackets is of order unity, which is the case for the latest generation of broadband interferometric gravitational-wave detectors.

To estimate the gravitational-wave amplitude of the strongest source requires a bit of care. To get the flavor of the original argument, consider a one-octave frequency band $[f, 2f]$. The quantity in square brackets in (2.7) is $15/16$, which we approximate as unity. Substituting the distance to the closest source (2.7) into (2.5) and neglecting the fact that $f^2$ can vary by up to a factor of four within the octave, gives the amplitude of the strongest source in this one-octave frequency band to be

$$h = 4\pi^2 \frac{GI}{c^4} \frac{\varepsilon f^2 \sqrt{\tau_{\rm GW}}}{R\sqrt{\tau_{\rm B}}} = 4\pi^2 \frac{GI}{c^4} \frac{\sqrt{\beta}}{R\sqrt{\tau_{\rm B}}} = \sqrt{\frac{5GI}{8c^3 R^2 \tau_{\rm B}}}. \tag{2.8}$$

The Blandford argument is simply the observation that this amplitude is (1) independent of the population's deformation $\varepsilon$ and (2) independent of frequency $f$.

Blandford's argument may also be stated in terms of a comparison between two different model Galaxies, each containing a similar populations of gravitars but each having a different (but constant) value of the ellipticity.

### B. Restating Blandford's argument

The previous paragraph is a rigorous version of Blandford's original argument. We now generalize this, building on the methods first presented in [2].

Let us first define useful quantities to describe a population of gravitars. As before $r$ denotes the distance between gravitar and detector, $f$ is the frequency of gravitational waves emitted, and $\varepsilon$ is the ellipticity of the gravitar.

In this section $t$ measures the age of the gravitars. A gravitar with age $t = 0$ is born at the present time, whereas $t > 0$ for a gravitar born in the past.

Because optimal mutual orientation of the gravitar's spin and the detector's normal axis is assumed, the gravitational-wave amplitude depends only on the distance $r$ but not on the sky position. Therefore, it is useful to define the probability $\mathrm{d}P_r$ of finding a gravitar born time $t$ ago at the present time in a spherically symmetric shell $[r, r + \mathrm{d}r]$ around the Sun [5]. The probability can be written in terms of a probability density $\varrho_r(r, t)$ as

$$\mathrm{d}P_r = \varrho_r(r, t)\mathrm{d}r. \tag{2.9}$$

Moreover, let us define the probability $\mathrm{d}P_f$ of finding gravitars born time $t$ ago with ellipticity $\varepsilon$ in a present-time frequency band $[f, f + \mathrm{d}f]$. $\mathrm{d}P_f$ can be written in terms of a probability density $\varrho_f(\varepsilon, f, t)$ as

$$\mathrm{d}P_f = \varrho_f(\varepsilon, f, t)\mathrm{d}f. \tag{2.10}$$

Note, that the probability densities are normalized by $\int_0^\infty \mathrm{d}r\varrho_r(r, t) = 1 \forall t$ and $\int_0^\infty \mathrm{d}f\varrho_f(\varepsilon, f, t) = 1 \forall \varepsilon, t$.

For further generalization consider a continuous distribution of gravitational-wave frequencies at birth instead of a single, high value. Let $\mathrm{d}P_{f_0}$ be the probability of the birth frequency being in a band $[f_0, f_0 + \mathrm{d}f_0]$. The corresponding probability density $\varrho_{f_0}(f_0)$ is defined by

$$\mathrm{d}P_{f_0} = \varrho_{f_0}(f_0)\mathrm{d}f_0, \tag{2.11}$$

normalized as before. Frequency change by redshift from cosmological evolution is neglected since all gravitars considered are within our galaxy.

To link the initial frequency distribution $\varrho_{f_0}$ to the present-time distribution $\varrho_f$, consider a gravitar with ellipticity $\varepsilon$ whose current frequency is $f$, and let $f_0(\varepsilon, f, t)$ denote the gravitar's frequency at time $t$ in the past. Solving (2.2) for the birth frequency yields

$$f_0(\varepsilon, f, t) = (f^{-4} - \beta^{-1}\varepsilon^2 t)^{-1/4}. \tag{2.12}$$

The probability density $\varrho_f$ can be rewritten in terms of the initial frequency distribution $\varrho_{f_0}$ by a change of variables. The fraction of gravitars in a birth frequency band $[f_0, f_0 + \mathrm{d}f_0]$ is the same as the fraction in a present-time frequency band $[f, f + \mathrm{d}f]$, so the identity $\varrho_f \mathrm{d}f = \varrho_{f_0}\mathrm{d}f_0$ yields

$$\varrho_f(\varepsilon, f, t)\mathrm{d}f = \varrho_{f_0}(f_0(\varepsilon, f, t)) \frac{\partial f_0(\varepsilon, f, t)}{\partial f}\mathrm{d}f \tag{2.13}$$

$$= \varrho_{f_0}(f_0(\varepsilon, f, t)) \frac{f_0^5(\varepsilon, f, t)}{f^5}\mathrm{d}f, \tag{2.14}$$

from which

$$\varrho_f(\varepsilon, f, t) = \varrho_{f_0}(f_0(\varepsilon, f, t)) \frac{f_0^5(\varepsilon, f, t)}{f^5} \tag{2.15}$$

immediately follows.

To allow for a time-dependent birthrate of galactic gravitars, let $\dot{n}(t)$ be the birthrate as a function of $t$. The number of gravitars $\mathrm{d}N$ formed during a short time interval $[t, t + \mathrm{d}t]$ is then $\mathrm{d}N = \dot{n}(t)\mathrm{d}t$.

The number $\mathrm{d}\tilde{N}$ of gravitars in a thin spherical shell $[r, r + \mathrm{d}r]$ around the position of the Sun, with frequencies in $[f, f + \mathrm{d}f]$, with fixed ellipticity $\varepsilon$, formed in a time interval $[t, t + \mathrm{d}t]$ ago is then given by

$$\begin{aligned} \mathrm{d}\tilde{N} &= \mathrm{d}P_r \times \mathrm{d}P_f \times \mathrm{d}N \\ &= \varrho_r(r, t)\mathrm{d}r \times \varrho_f(\varepsilon, f, t)\mathrm{d}f \times \dot{n}(t)\mathrm{d}t. \end{aligned} \tag{2.16}$$

From (2.5), it follows that for fixed $\varepsilon$ and $f$ there is a unique, invertible mapping $r(h)$ from the amplitude of gravitational waves $h$ to the distance $r$ of the gravitar from the Sun. A change of variables from $r$ to $h$ yields

$$\mathrm{d}\tilde{N} = \varrho_r(r(h), t)\frac{\mathrm{d}r(h)}{\mathrm{d}h}\mathrm{d}h \times \varrho_f(\varepsilon, f, t)\mathrm{d}f \times \dot{n}(t)\mathrm{d}t, \tag{2.17}$$

and the number $M(f_1, f_2, h_{\rm max})$ of gravitars with a gravitational-wave amplitude $h \geq h_{\rm max}$ in a frequency band $[f_1, f_2]$ and ages $t \leq \bar{t}$ is given by integration as

$$\begin{aligned} M(f_1, f_2, h_{\rm max}) = &\int_0^{\bar{t}} \mathrm{d}t\dot{n}(t) \int_{f_1}^{f_2} \mathrm{d}f\varrho_f(\varepsilon, f, t) \\ &\times \int_{h_{\rm max}}^{\infty} \mathrm{d}h\varrho_r(r(h), t)\frac{\mathrm{d}r(h)}{\mathrm{d}h}. \end{aligned} \tag{2.18}$$

Here, the integral over $h$ is performed for a fixed $\varepsilon$ (assuming the same ellipticity for every gravitar) and fixed $f$ and $t$. After integrating out the dependence on $h$ the followup integration over $f$ weights the previous integral by the

frequency density. The last integration sums the distributions from different birth times weighted by the galactic neutron star birthrate at that time.

Before Eq. (2.18) is used to rederive Blandford's result, let us prove that the frequency distribution from a single birth frequency has reached a steady state ($\partial_t \varrho_f = 0$) at frequency $f$, if $f(t) < f < f_B$, where $f(t)$ is given by (2.2). Consider a frequency band $[f,\ f + \mathrm{d}f]$, which is wide enough to contain at least one gravitar at all times $t$. If $f(t) < f < f_B$, the constancy of the birthrate guarantees that if and only if a gravitar leaves the frequency band by the lower boundary, another gravitar will enter the frequency band from higher frequencies. The assumption of a steady state is crucial. If the distribution has not reached a steady state in a certain frequency band, there will be no sources in that band, and there is no contribution to the integral in (2.18).

Let us now rederive Blandford's result by using a density function $\varrho_r(r, t) = 2r/R^2$, which describes a population of galactic gravitars uniformly distributed in a flat two-dimensional disk with radius $R$ [6]. Further, assume a constant birthrate $\dot{n}(t) = \frac{1}{\tau_B}$ and a single high birth frequency $f_B$ such that $\varrho_{f_0}(f_0) = \delta(f_0 - f_B)$. Inserting $r(h)$ into (2.18) by solving (2.5) for $r$, we find after a slightly technical but straightforward calculation

$$M(f_1, f_2, h_{\max}) = \frac{5GI}{\tau_B c^3 R^2} \int_{f_1}^{f_2} \frac{\mathrm{d}f}{f} \int_{h_{\max}}^{\infty} \frac{\mathrm{d}h}{h^3}. \tag{2.19}$$

The integrations are trivial and yield

$$M(f_1, f_2, h_{\max}) = \frac{5GI}{2\tau_B c^3 R^2} h_{\max}^{-2} \ln\left(\frac{f_2}{f_1}\right). \tag{2.20}$$

Let us follow [2] and assume a 50% chance of detection, corresponding to $M = 1/2$. One finds a maximum gravitational-wave strain [2]

$$h_{\max} = \sqrt{\frac{5GI}{\tau_B c^3 R^2} \ln\left(\frac{f_2}{f_1}\right)}. \tag{2.21}$$

This result can also be directly compared with the earlier result (2.8) from the cruder analysis, by setting $f_2 = 2f_1$ and setting $M = 1$. The values of $h_{\max}$ obtained by these two different analyses disagree by about 40%, but are independent of deformation and frequency $f_1$.

For a broadband search performed today, we assume $\ln(f_2/f_1) \approx 1$. Then (2.21) gives the largest amplitude expected under the assumptions [7] from galactic gravitars as $h_{\max} \approx 10^{-24}$.

For later comparison with the realistic galactic model, let us calculate the dimensionless averaged fractional frequency density $\hat{\varrho}_f(\varepsilon, f)$ in the population. It is defined by $\mathrm{d}\hat{P}_f = \hat{\varrho}_f(\varepsilon, f)\frac{\mathrm{d}f}{f}$ being the probability to find gravitars with a fixed ellipticity $\varepsilon$ in a frequency band $[f,\ f + \mathrm{d}f]$,

$$\hat{\varrho}_f(\varepsilon, f) = \frac{f}{N_{\mathrm{tot}}} \int_0^{\bar{t}} \mathrm{d}t \dot{n}(t) \varrho_f(\varepsilon, f, t), \tag{2.22}$$

where $N_{\mathrm{tot}} = \int_0^{\bar{t}} \mathrm{d}t\ \dot{n}$ is the number of gravitars formed during the timespan $\bar{t}$. Using the same assumptions as for the derivation of (2.20) yields

$$\hat{\varrho}_f(\varepsilon, f) = \frac{4\beta}{\tau_B} \varepsilon^{-2} f^{-4}. \tag{2.23}$$

For fixed ellipticity the averaged fractional frequency density falls off with $f^{-4}$ and scales for fixed frequency as $\varepsilon^{-2}$.

Let us summarize the assumptions made for this analytic calculation of the strongest gravitational-wave signal from galactic gravitars. Assume all gravitars are born at a single high birth frequency with fixed ellipticity and constant birthrate, and reside in a two-dimensional, uniform distribution, i.e. in a thin galactic disk. Assume their spin-down is governed by the emission of gravitational waves as described by Eq. (2.2). Adopting these assumptions and a 50% chance of actual detection, the largest amplitude $h_{\max}$ of gravitational waves emitted by galactic gravitars in a frequency band $[f_1, f_2]$ is given by (2.21). Thus, a precise statement about $h_{\max}$ is the following

*Result*: Assume the existence of a population of galactic gravitars with uniform, two-dimensional spatial distribution, single, high birth frequency, fixed ellipticity $\varepsilon$, and constant birthrate. Choose a frequency band $[f,\ sf]$ with scale $s > 1$ large enough such that there is at all times at least one gravitar in this band. Then the largest amplitude $h_{\max}$ of gravitational waves emitted by galactic gravitars in this band is independent of $f$ and $\varepsilon$ and depends only on the scale $s$.

Searching wider ranges of frequencies increases the value of $h_{\max}$, because the absolute number of gravitars in wider ranges of frequency increases. However, in (2.21) the gain from going to higher frequencies grows slowly, as the square root of the logarithm, because the gravitars spend less time at higher frequencies.

### C. A natural limit to the result

Because of the crucial assumption of a steady-state distribution in frequency, there are obvious limits to this simple model. The time to reach a steady state in a given narrow frequency band $[f,\ f + \mathrm{d}f]$ must be at least of the same order of magnitude as the spin-down timescale (2.4), because otherwise no gravitar will have spun down to frequencies contained in the band.

If all gravitars are born at the same high frequency the time to reach a steady state is exactly the spin-down age. If on the other hand, there is a continuous distribution of initial frequencies, then reaching a steady state in a certain frequency band requires longer evolution times. Only then most of the gravitars in that band are ones that have spun down from higher frequencies. Over time this effect

"washes out" any effects of the initial frequency distribution.

There is a natural limit to the result due to the finite age of the Universe, since no gravitar can be older than the Universe itself. An even better limit would be the age of the Galaxy, or rather that of the galactic neutron star population. However, since the age of the Universe is known much more accurately than the age of the Galaxy, and since they differ only by a factor of order 2, we will use the age of Universe in all of our estimates below.

The age of the Universe $t_0$ can be calculated from Hubble's constant $H_0$ as $t_0 = \frac{2}{3}H_0^{-1}$. Then the finiteness sets limits on the values of $\varepsilon$ and $f$ for which the population has reached a steady state. We easily find from (2.4) that the population is in a steady state for gravitational-wave frequencies that satisfy

$$\varepsilon^2 f^4 > \frac{3}{2} H_0 \beta. \tag{2.24}$$

Fixing the ellipticity, one can calculate a frequency

$$\tilde{f}(\varepsilon) = \left(\frac{3H_0\beta}{2\varepsilon^2}\right)^{1/4} = 76\ \mathrm{Hz}\left(\frac{10^{-7}}{\varepsilon}\right)^{1/2} \tag{2.25}$$

above which the population can be assumed to be close to a steady state.

We would like to stress that a realistic population with a continuous distribution of initial frequencies has to have evolved over a time $T \approx$ few $\times\, \tau_{\mathrm{GW}}$ to be in steady state. Thus, the true value of $\tilde{f}(\varepsilon)$ is larger by a factor of a few, and falls into the frequency range of highest sensitivity in modern interferometric gravitational-wave detectors (between 100 Hz and 300 Hz).

The range of ellipticities for which the assumption of steady state breaks down is then given by

$$\tilde{\varepsilon}(f) \lesssim 5.8 \times 10^{-8}\left(\frac{100\ \mathrm{Hz}}{f}\right)^2. \tag{2.26}$$

In general, it is not valid to assume that the frequency distribution in our galaxy is in steady state.

We postpone further discussion of a uniform two-dimensional spatial distribution to Sec. IV C after presenting the setup of our numerical galactic model.

## III. NUMERICAL MODEL

The second section of this paper gave a precise analytic formulation of Blandford's argument including the extensions and improvements of Ref. [2]. To understand if this argument holds in a more realistic model of our galaxy, we set up a numerical simulation of the time evolution of a population of galactic gravitars. This follows [3], using a more recently published result [8] for the initial velocity distribution of neutron stars. To compute the spatial distribution, the equations of motion following from the Galactic potential given in Sec. III A are evolved over time. The assumed initial conditions for the differential equations (i.e. initial positions and velocities of the gravitars) are described in Secs. III B and III C respectively. Section III D describes the adopted distributions for the initial spin period. The results of the simulations will be presented afterwards in Secs. IV A and IV B.

### A. Galactic potential and equations of motion

The motion of Galactic gravitars is governed by the galactic gravitational potential. The potential first given by Paczynski [9] is adopted. This potential describes our galaxy as axisymmetric with respect to the rotation axis. Thus, cylindrical coordinates $\rho$, $z$, and $\varphi$ are used. $\rho$ denotes the distance to the galactic rotation axis, and $z$ is the distance perpendicular to the disk.

The adopted potential represents our galaxy as composed of three different mass components. The most massive is a nonuniform flat disk with a radial scale of 3.7 kpc and a $z$-direction scale of 0.2 kpc. The component with the second highest mass is the halo, which is described by a density distribution $\varrho_{\mathrm{H}} \propto (r^2 + r_{\mathrm{H}}^2)^{-1}$, where $r_{\mathrm{H}} = 6$ kpc is called the halo core radius. The central bulge of our galaxy is represented by a spheroidal lower mass component with a density $\varrho_{\mathrm{S}} \propto (r^2 + b_{\mathrm{S}}^2)^{-5/2}$, where $b_{\mathrm{S}} = 0.277$ kpc.

The corresponding potential therefore consists of three terms

$$\Phi(\rho, z) = \Phi_{\mathrm{S}}(r) + \Phi_{\mathrm{D}}(\rho, z) + \Phi_{\mathrm{H}}(r), \tag{3.1}$$

describing, respectively, the potential energy per unit mass of the spheroid, the disk and the halo in our galaxy. The first two components ($i = \mathrm{S}, \mathrm{D}$) are given by

$$\Phi_i(\rho, z) = -GM_i\left[\rho^2 + \left(a_i + \sqrt{z^2 + b_i^2}\right)^2\right]^{-1/2}. \tag{3.2}$$

For the potential of the halo $r^2 = \rho^2 + z^2$ is substituted and the following spherical symmetric expression is used

$$\Phi_{\mathrm{H}}(r) = \frac{GM_{\mathrm{H}}}{r_{\mathrm{H}}}\left[\frac{1}{2}\ln\left(1 + \frac{r^2}{r_{\mathrm{H}}^2}\right) + \frac{r_{\mathrm{H}}}{r}\arctan\left(\frac{r}{r_{\mathrm{H}}}\right)\right]. \tag{3.3}$$

The parameter values are shown in Table I.

The axial symmetry of the galactic model leads to conservation of the $z$ component of the angular momentum $L_z$. Thus, the effective potential is

$$\Phi_{\mathrm{eff}}(\rho, z) = \Phi(\rho, z) + \frac{L_z^2}{2\rho^2}. \tag{3.4}$$

The equations of motion that are evolved are

$$\ddot{\rho} = -\frac{\partial \Phi_{\mathrm{eff}}}{\partial \rho} \quad \text{and} \quad \ddot{z} = -\frac{\partial \Phi_{\mathrm{eff}}}{\partial z}. \tag{3.5}$$

The equation of motion for $\varphi$ is given by $\rho^2\dot{\varphi} = L_z$. In the simulation, this equation is not used because $\varphi$ is not evolved, but drawn from a uniform random distribution $\varphi \in [0, 2\pi)$.

TABLE I. Mass and scale parameters for the galactic potential

| | | | |
|---|---|---|---|
| *Disk*: | $M_{\mathrm{D}} = 8.07 \times 10^{10} M_{\odot}$ | $a_{\mathrm{D}} = 3.7$ kpc | $b_{\mathrm{D}} = 0.200$ kpc |
| *Spheroid*: | $M_{\mathrm{S}} = 1.12 \times 10^{10} M_{\odot}$ | $a_{\mathrm{S}} = 0$ kpc | $b_{\mathrm{S}} = 0.277$ kpc |
| *Halo*: | $M_{\mathrm{H}} = 5.00 \times 10^{10} M_{\odot}$ | $r_{\mathrm{H}} = 6.0$ kpc | |

### B. Initial spatial distribution

The initial spatial distribution of gravitars is proportional to the density of massive progenitor stars of neutron stars. While there is quite good agreement about the initial distribution in $z$ direction, the initial distribution along the radial direction is unknown.

In the $z$ direction, the initial position is drawn from a Laplacian distribution with scale factor $z_0 = 0.075$ kpc. The probability of a gravitar's birth in an interval $[z, z + \mathrm{d}z]$ is given by

$$p_z(z)\mathrm{d}z = \frac{1}{2z_0} \exp\left(-\frac{|z|}{z_0}\right)\mathrm{d}z. \tag{3.6}$$

We considered three different models for the initial radial distribution together with the given initial $z$ distribution.

To illustrate the expected distance to the strongest gravitars we used the results of Fig. 5 together with Eq.(2.5) to compute the distance to these sources as a function of the gravitational-wave frequency interval and the ellipticity. The result is shown in Fig. 6.

The simplest radial distribution [from Ref. [3]] is an exponential falloff with a scale factor $\rho_1 = 3.2$ kpc. The probability of a gravitar's birth in a distance interval $[\rho, \rho + \mathrm{d}\rho]$ is then

$$p_1(\rho)\mathrm{d}\rho = \frac{1}{\rho_1} \exp\left(-\frac{\rho}{\rho_1}\right)\mathrm{d}\rho. \tag{3.7}$$

Note however that this distribution leads to an extreme concentration of neutron stars towards the galactic center. These are not seen in pulsar surveys [10]. So following [9] a gamma distribution given by

$$p_2(\rho)\mathrm{d}\rho = a_\rho \frac{\rho}{\rho_2^2} \exp\left(-\frac{\rho}{\rho_2}\right)\mathrm{d}\rho, \tag{3.8}$$

is also considered, where gravitar formation in the disk is allowed for $\rho_3 \leq 25$ kpc, and the constants are given by $\rho_2 = 4.78$ kpc and $a_\rho = 1.0345$. A third distribution

$$p_3(\rho)\mathrm{d}\rho = \frac{\rho^5}{120\rho_3^6} \exp\left(-\frac{\rho}{\rho_3}\right)\mathrm{d}\rho, \tag{3.9}$$

with $\rho_3 = 1.25$ kpc taken from [10] is also considered. It is fitted to the radial distribution of Population I stars, which are considered to be likely progenitors of neutron stars. Again, gravitar birth events are allowed for $r \leq 25$ kpc. On average, only one gravitar out of 14 thousand is born with $\rho > 25$ kpc, so the normalization constant $a_\rho \approx 1$.

### C. Initial velocity

The galactic rotation determines the velocity of the supernova progenitors and therefore also that of the newborn neutron stars.

From classical mechanics the rotational speed of a body on a circular orbit in the axisymmetric potential (3.1) is given by $v_{\mathrm{rot}} = \sqrt{\rho \partial_\rho \Phi(\rho, z)}$. From the initial coordinate of a gravitar the corresponding $v_{\mathrm{rot}}$ on a tangential circular orbit is calculated (neglecting initial rotation velocities perpendicular to the galactic disk, because all gravitars are born with low initial values of $z$). Looking down on the Galaxy from positive $z$ values the Galaxy is chosen to rotate counterclockwise.

Furthermore, it is assumed that gravitars are born in a supernova explosion that will kick the newborn star. The direction of that kick is assumed to be isotropic. The kick speed is drawn from a Maxwellian distribution with a mean velocity $\bar{v} = 430$ km/s. The probability for the kick speed to be in an interval $[v_{\mathrm{kick}}, v_{\mathrm{kick}} + \mathrm{d}v_{\mathrm{kick}}]$ is

$$p_v(v_{\mathrm{kick}})\mathrm{d}v_{\mathrm{kick}} = \frac{32 v_{\mathrm{kick}}^2}{\pi^2 \bar{v}^3} \exp\left(-\frac{4 v_{\mathrm{kick}}^2}{\pi \bar{v}^2}\right)\mathrm{d}v_{\mathrm{kick}}. \tag{3.10}$$

It is assumed that this distribution from Ref. [8] may be used for gravitars as well as for pulsars.

### D. Initial period distribution

Because of the conservation of angular momentum in the supernova event and the much smaller radius of the gravitar compared with its progenitor, newborn neutron stars will spin rapidly.

We considered three models for the distribution of the initial rotation periods following the models given in Ref. [3]. The existence of three different models reflects our ignorance of the actual distribution of initial periods.

The first model is described by a lognormal distribution

$$p_{P_0}(P_0) = \frac{1}{\sqrt{2\pi}\sigma P_0} \exp\left[-\frac{1}{2\sigma^2}(\ln(P_0) - \ln(\bar{P}_0))^2\right], \tag{3.11}$$

where $P_0$ is measured in seconds and where the values $\sigma = 0.69$ and $\bar{P}_0 = 5$ ms are taken from Ref. [11]. Gravitars with $P_0 < 0.5$ ms are excluded.

The second model is using the same probability distribution as the first model, but every initial period $P_0 < 10$ ms is set to 10 ms exactly. In this way the possible presence of $r$-modes in young neutron stars is mimicked. These modes can dissipate rotational energy of the new-

born neutron star and increase its initial period to about 10 ms within 1 yr.

The third model considered is a further extension of the second one. It includes the effects of matter fallback after the supernova explosion. The increase of angular momentum by the accreting matter could counteract the $r$-mode induced deceleration. The resulting initial period will approach an intermediate value. The choice from [3] to draw the initial period from a uniform distribution between 2 ms and 15 ms is adopted.

### E. Coding and implementation

With the initial distributions from Secs. III B and III C and the equations of motion (3.5) at our disposal, it is a straightforward problem to find the spatial distribution of a population of gravitars at the present time.

The code for the simulation is written in *C*. The equations of motion (3.5) are integrated via a Burlisch-Stoer method in combination with Stoermer's rule for the direct discretization of a system of second-order differential equations using routines described in [12]. Over the integration time the total energy is conserved to one part in $10^6$.

For the derivation of the frequency distributions (2.15) the probability distributions are implemented by random number generators and functions from the GNU Scientific Library (GSL) [13]. The fractional frequency density (2.22) is obtained via a Monte Carlo integration using $2 \times 10^{12}$ random values of initial frequency and a uniform distribution of ages.

Depending on the model of the initial spatial distribution the integration of $10^6$ neutron star trajectories over a time of 200 Myrs takes 2.5 mins to 13.3 mins on an AMD Opteron 185 processor. Most of the simulations were done on the Morgane cluster at the AEI in Potsdam.

## IV. RESULTS

### A. Frequency distributions

In the derivation of the generalized result (2.19) the assumption of a steady-state frequency distribution (2.23) is (along with the two-dimensional uniform spatial distribution) the key to the independence of the maximum amplitude on ellipticity and frequency. Let us therefore first have a look at the frequency distributions that result from a continuous distribution of initial frequencies and compare them with the corresponding density resulting from a single birth frequency (2.23).

Figure 1 shows the results of the Monte Carlo integration for $\bar{t} = 13.6$ Gyrs using a lognormal distribution of initial periods and a fixed ellipticity for each run in the frequency range $f \in [50\ \mathrm{Hz}, 2000\ \mathrm{Hz}]$. The ellipticity varies over 3 orders of magnitude from $10^{-9}$ to $10^{-6}$. The dashed lines correspond to a scaling proportional to $f^{-4}$, which results from a single birth frequency and shows a steady-state distribution as calculated in Eq. (2.23).

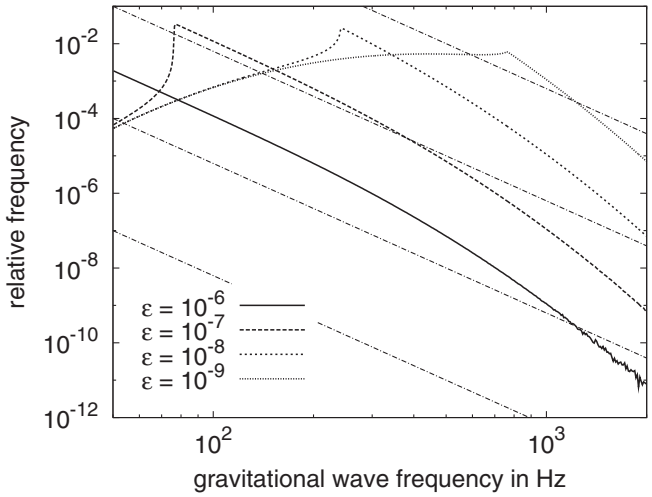


FIG. 1. The distribution $\hat{\varrho}_f(\varepsilon, f)$ in frequency after $\bar{t} = 13.6$ Gyrs for varying ellipticity using a lognormal distribution of initial periods in the range $f \in [50\ \mathrm{Hz}, 2000\ \mathrm{Hz}]$. The dashed lines correspond to a slope $f^{-4}$, as Eq. (2.23) would predict for a single high birth frequency. The kink in the graphs for $\varepsilon \lesssim 10^{-7}$ is at the frequency given by Eq. (2.25).

For $\varepsilon = 10^{-6}$ the population is close to a steady state at the present time, because the scaling is nearly proportional to $f^{-4}$. For smaller ellipticities, one can identify a kink in the density function at a frequency $\tilde{f}$ as given by (2.25). The kink is due to gravitars born at high frequencies that are too young to have spun down to lower frequencies. The frequency distribution for $\varepsilon \lesssim 10^{-7}$ is not in a steady state in the frequency range of highest sensitivity for modern interferometric detectors, which is between 100 Hz and 300 Hz.

We also note that $\hat{\varrho}_f(\varepsilon, f)$ does not scale as $\varepsilon^{-2}$ in all frequency bands. It only scales as $\varepsilon^{-2}$ at high frequencies.

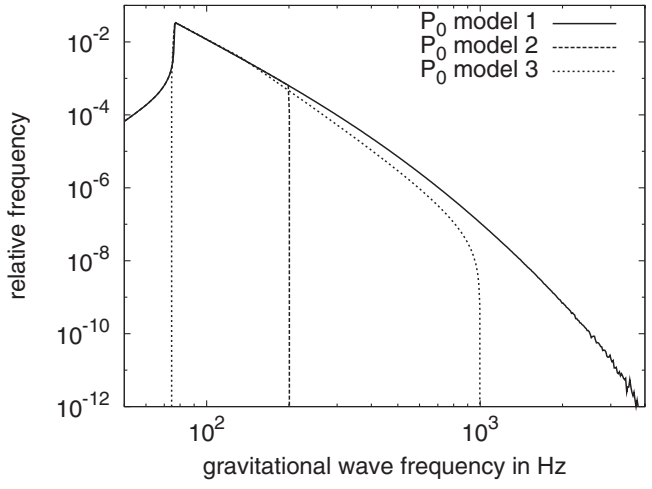


FIG. 2. The distribution in frequency space in the range $f \in [50\ \mathrm{Hz}, 4000\ \mathrm{Hz}]$ after $\bar{t} = 13.6$ Gyrs for $\varepsilon = 10^{-7}$ for three different models of the initial gravitar frequency distribution.

Let us now compare the fractional frequency densities that result from different models of initial frequency distributions for a fixed ellipticity. Figure 2 shows the distribution in frequency space after an evolution time of $\bar{t} = 13.6$ Gyrs for $\varepsilon = 10^{-7}$. Each graph corresponds to one of the models for the initial frequency distribution.

If the evolution time is long compared with the spin-down time $\tau_{\mathrm{GW}}$ (2.4), most of the gravitars will have spun down to low frequencies, and the distribution will be dominated by those older sources. Yet, if the respective model has upper or lower limits on the birth frequencies, one cannot expect the fractional densities to agree near these boundaries. However, in frequency bands of interest for modern interferometric detectors (100 Hz to 300 Hz) the distributions only show minor differences between the different models.

### B. Spatial steady-state distribution and timescales

Since the gravitars are born in a thin disk and receive an isotropic kick by the supernova, they tend to leave the disk after some Myrs. They either escape the galactic gravitational potential, or are bound to the Galaxy on some ''orbit.'' The numerical simulation is used to find the timescale on which these processes wash out the imprint of the initial spatial distribution.

Let us introduce the function $\hat{M}(r, t)$, which is the number of gravitars in a ball of radius $r$ around the position of the Sun that were formed a time $t$ ago. The radial probability distribution $\varrho_r(r, t)$ as introduced in Sec. II B is related to $\hat{M}$ via the derivative with respect to $r$

$$\varrho_r(r, t)\mathrm{d}r = \frac{1}{N_{\mathrm{tot}}}\partial_r \hat{M}(r, t)\mathrm{d}r. \tag{4.1}$$

To obtain a dynamical picture, $\hat{M}(r, t)$ is computed in steps of 1 Myr from 0 Myrs to 200 Myrs. For each of the 201 values of integration time the trajectories of $N_{\mathrm{tot}} = 10^9$ galactic gravitars are evolved using the numerical integration methods described in Sec. III E, and the radial distance distribution is derived from their final positions. The radial resolution is chosen as 2.5 pc for 0 kpc $\leq r <$ 12 kpc and as 100 pc for 12 kpc $\leq r \leq$ 20 kpc.

Figure 3 shows the number of gravitars inside balls of radius $r$ around the position of the Sun, which were formed $t = 200$ Myrs ago for the different initial radial distributions. The saturation near $r = 8.5$ kpc is due to the high density of gravitars near the galactic center.

The simulations show that the spatial distribution settles into a state of equilibrium for $t \approx 200$ Myrs. There is no significant difference between the distributions for $t =$ 200 Myrs and $t = 2$ Gyrs. By the age of 200 Myrs the initial distribution is washed out; evolution over longer times no longer changes the radial distribution $\hat{M}(r)$.

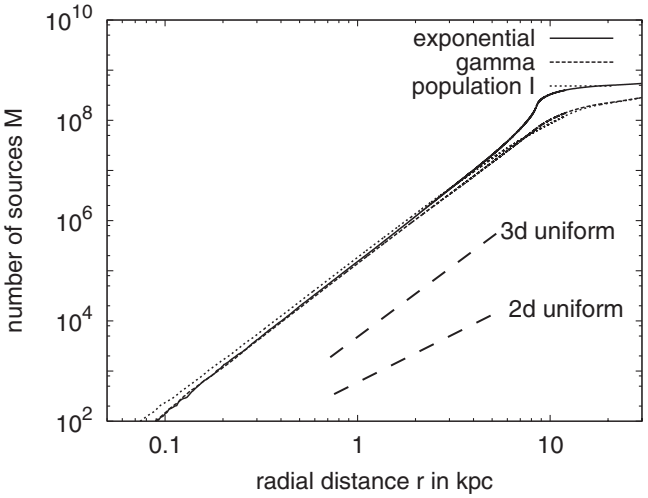


FIG. 3. The distribution of gravitars as a function of radial distance from the Sun. The graphs show the number of gravitars inside spheres of radius $r$ plotted against $r$. The age of all sources is $t = 200$ Myrs. The scaling dimension of these graphs is shown in Fig. 4. The straight (dashed) lines show the corresponding slope for a uniform two- (three-) dimensional distribution.

### C. Scaling dimension of the spatial distribution

The assumption of a two-dimensional and uniform spatial distribution of gravitars at the present time is crucial for Blandford's argument. The numerical simulation can test if these assumptions are valid or not.

A useful concept is that of the *scaling dimension*. To obtain the scaling dimension, the function $\hat{M}(r)$ as introduced in the previous section is used. Assume a uniform distribution, and describe the number of sources inside each ball as a function of its radius $r$ by a simple power law

$$\hat{M}(r) \propto r^D. \tag{4.2}$$

$D$ is called the scaling dimension of the distribution.

Even an exactly two-dimensional spatial distribution of gravitars (e.g. the galactic disk) can effectively scale as a $D$-dimensional object due to density gradients. Note that the scaling dimension is a local quantity depending on the position of evaluation.

To illustrate the scaling properties of the evolved galactic spatial distribution of gravitars, the local scaling dimension is computed for $r \leq 8$ kpc and is shown in Fig. 4. From (4.2) the scaling dimension $D(r)$ can be derived via

$$D(r) = \frac{r\partial_r \hat{M}(r)}{\hat{M}(r)} \tag{4.3}$$

The differentiation is computed numerically using a cubic splining on the tabulated values.

The scattering of points for $r \lesssim 1$ kpc is due to the small number of sources at short distances and resulting numerical noise.

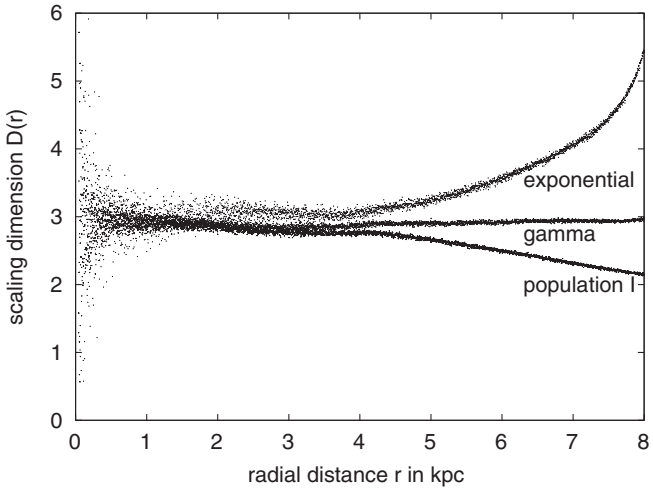


FIG. 4. The local scaling dimension $D(r)$ of the spatial distribution of gravitars around the position of the Sun as calculated by (4.3). The corresponding radial distributions of sources are shown in Fig. 3. Note, that here the graphs are only shown for $r \leq 8$ kpc.

The scaling dimension at every distance to the Sun is greater than 2. For the first model of initial radial distributions it even reaches values $D \geq 5$. For the second model there is a slight increase in the scaling dimension toward the galactic center, where the scaling dimension $D \approx 3$. For the last model the scaling dimension decreases with larger radial distance but always $D > 2$.

We conclude that the scaling dimension of the population of gravitars in the model of our galaxy is significantly larger than 2. More precisely averaging $D$ over distances $r \leq 2$ kpc—where $D$ is nearly constant and independent of the initial radial distribution—yields $D \approx 2.95$.

## V. THE STRONGEST CONTINUOUS GRAVITATIONAL-WAVE SIGNAL

Using the frequency and spatial distributions obtained from our galactic simulation, it is straightforward to derive the maximum expected amplitude of continuous gravitational waves from gravitars.

### A. Numerical method

Let us first describe the numerical method for computing the maximum expected amplitude of the gravitational waves using the distributions in space and frequency as presented in Secs. IV A and IV B.

Equation (2.18) is used to obtain the value of $M(f_1, ef_1, h_{\max})$ for a given frequency band $[f_1,\ ef_1]$ ($\ln(e) = 1$) and a trial value of $h_{\max}$. To compare the results with Ref. [2] $h_{\max}$ is tuned via a bisection method within $\pm 2.5\%$ to the target value $M_{\text{tar}} = 0.5$ such that $0.4875 \leq M(f_1, ef_1, h_{\max}) \leq 0.5125$.

As described in Sec. IV B the function $\hat{M}(r, t)$ giving the number of gravitars with a solar radial distance less than $r$ is tabulated. From these values $\varrho_r(r, t) = \partial_r \hat{M}(r, t)/N_{\text{tot}}$ is numerically computed via a cubic splining method.

The distribution in frequency space $\varrho_f(\varepsilon, f, t)$ is taken from Eq. (2.15) with distributions of initial periods as described in Sec. III D.

Given a frequency band a high value of $h_{\max}$ is chosen as trial value. Then the frequency is chosen fixed at the lower boundary of the band and the integration over $h \in [h_{\max}, h_{\text{up}}]$ in (2.18) is conducted by calculating from (2.5) the corresponding $r(h)$ and inserting into the interpolated $m(r, t)$. For the upper limit $h_{\text{up}}$ of the integration the value that would obtained if the gravitar was at the closest possible distance is taken. Then no contribution to the integral is lost. After integrating over $h$ the integration over frequency in the chosen band $[f_1,\ ef_1]$ is done and weighted by $\varrho_f(\varepsilon, f, t)$.

The result of these two integrations is then integrated over all times $t \in [0, \bar{t} = 13.6\ \text{Gyrs}]$, where the timestep between two evaluations is chosen as $\mathrm{d}t = \min\{1\ \text{M yr}, \frac{\tau_{gw}}{10}\}$ to obtain a sufficiently fine timestep to track both spatial and frequency evolution. This integration over time is weighted by a constant birthrate of $\dot{n}(t) = (30\ \text{yrs})^{-1}$.

### B. Maximum expected amplitude

Using the results of the simulation, one can see if the value of $h_{\max}$ (obtained by the method described in the previous section) differs from the one predicted by Blandford's result as extended and improved in Ref. [2].

To avoid boundary effects, from now only the first model for the distribution of initial frequencies is considered. In all frequency bands, the other models always give a smaller maximum amplitude of gravitational waves $h_{\max}$.

Figure 5 shows the resulting value of $h_{\max}$ for different values of the ellipticity and all spatial distribution models. The graphs are to be understood as follows: the maximum amplitude of gravitational waves is calculated as described in the previous section for every choice of initial spatial distributions and for frequency bands $[f,\ ef]$. The graphs shows the value $h_{\max}$ obtained in such a band as a single point at $(f, h_{\max})$.

From Fig. 5 it is obvious that the assumptions of Blandford's argument are not fulfilled for a realistic model of our galaxy. The graphs for different values of ellipticity do not line up, and each single graph is curved. Thus, the maximum amplitude of gravitational waves from galactic gravitars does depend on both the ellipticity and frequency.

For highly deformed gravitars, the graphs are nearly flat indicating a weak dependence on $f$, while for low values of $\varepsilon$ the previously discussed kink appears.

The choice of the initial radial distribution causes only small differences. The intermodel differences are usually of the order of 10%, and in the worst case are about 50% for a particular ellipticity and frequency. This is because the strongest gravitational waves are emitted by gravitars at

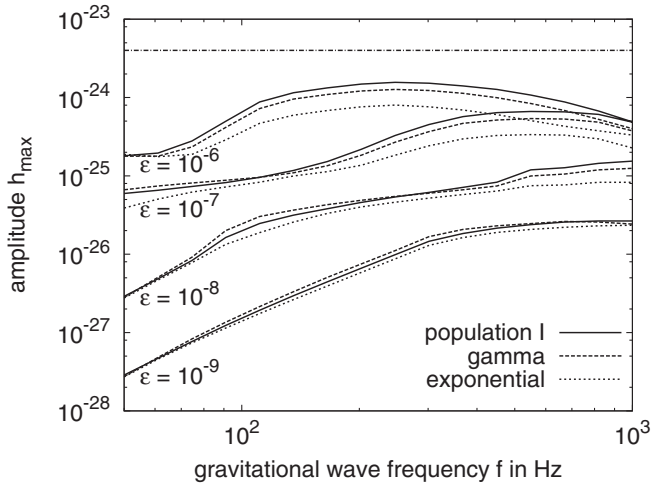


FIG. 5. The maximum strain amplitude of gravitational waves $h_{\max}$ from galactic gravitars in frequency bands $[f, ef]$ in the range $f \in [50\ \text{Hz}, 1000\ \text{Hz}]$. Each plotted point $h_{\max}(f)$ is the value $h_{\max}$ calculated for a frequency band $[f, ef]$, which is one natural-logarithmic-octave wide. The three curves show different initial spatial distribution models. For contrast, the dotted, straight line (independent of frequency and ellipticity $\varepsilon$) shows the value of $h_{\max}$ from [2], which improved and extended Blandford's argument.

very small distances [14]. As can be seen from Fig. 3, the distribution for radial distances $r \lesssim 5$ kpc from the Sun is nearly the same independent of the initial radial distribution.

Assuming the highest possible ellipticity $\varepsilon = 10^{-6}$ for the gravitars, the strongest signal has an amplitude of

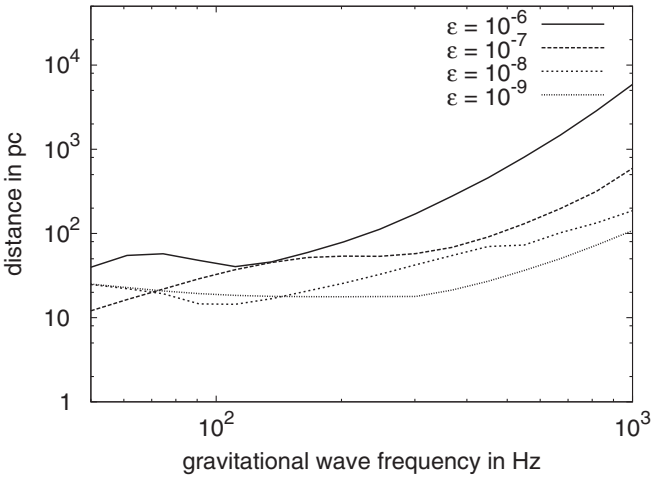


FIG. 6. The expected distance to the strongest gravitar, corresponding to Fig. 5. Because each frequency axis value of Fig. 5 refers to an entire logarithmic octave $\ln(f_2/f_1) = 1$ range, in principle the plots should show a range of distances that is two logarithmic octave wide: $\ln(h_2/h_1) = 2$. To simplify the appearance of this plot, we show only a single curve at the central value. The expected range of distances ranges from a factor of $1/e$ below this plot to $e$ above this plot.

TABLE II. Maximum values for the amplitude $h_{\max}$ of gravitational waves in dependence on the ellipticity $\varepsilon$.

| $\varepsilon$ | $h_{\max}$ | Frequency band |
|---|---|---|
| $10^{-6}$ | $1.6 \times 10^{-24}$ | [250 Hz, 680 Hz] |
| $10^{-7}$ | $6.6 \times 10^{-25}$ | [550 Hz, 1500 Hz] |
| $10^{-8}$ | $1.5 \times 10^{-25}$ | [1000 Hz, 2800 Hz] |
| $10^{-9}$ | $2.7 \times 10^{-26}$ | [1000 Hz, 2800 Hz] |

$h_{\max} \approx 1.6 \times 10^{-24}$ in the band [250 Hz, 680 Hz], which is improved (strengthened) by a factor of $\approx 3$ compared with the value given in [2]. Note that this improvement factor would be smaller if larger values of $\varepsilon$ were considered. In any case, the improvement factor is substantially larger at other frequencies.

In the case of the more realistic value $\varepsilon = 10^{-7}$, the estimate is $h_{\max} \approx 6.6 \times 10^{-25}$ in the band [550 Hz, 1500 Hz] and is lower than the simple analytic estimate by a factor of 6.

Table II lists the maximum values for the amplitude of the strongest gravitational waves for all adopted values of the ellipticity and the frequency band in which the maximum amplitude is expected.

To illustrate the expected distance to the strongest gravitars we used the results of Fig. 5 together with Eq. (2.5)to compute the distance to these sources as a function of the gravitational-wave frequency interval and the ellipticity. The result is shown in Fig. 6.

We conclude that the assumptions of Blandford's argument do not hold in our galactic model. The expected gravitar spatial distribution is not a two-dimensional uniform thin disk, and the expected gravitar frequency distribution is not yet in steady state for realistic values of neutron star ellipticity.

### C. Remarks on an upper limit

In the previous section, we obtained the expected maximum amplitude of a gravitational-wave signal from a deformed neutron star spinning down purely by gravitational waves. Let us now address the question whether this value poses an upper limit on the gravitational-wave amplitude from objects that spin down partly by gravitational waves and partly by electromagnetic dipolar emission. It must be stressed that recycled millisecond pulsars are not covered here, since spin-up is *not* considered.

Reference [2] gave a clever argument about why the expected maximum gravitational-wave strain from gravitars sets an upper limit for all neutron stars that have not gone through an accretion-powered spin-up phase. However, that argument implicitly assumes only birth frequencies *above* the observed frequency band for the pulsars, and also assumes that the pulsar population frequency-space distribution is in steady state in the observed frequency band. Here, we do not make either of these assumptions.

In this section we show that the results from Fig. 5 are a strict upper limit for frequencies $f > 250$ Hz. This is related to the distribution of initial frequencies, which has its maximum at $f_0 = 250$ Hz and is decreasing monotonically for larger values of initial frequency. To maximize the number of sources in a frequency band at a given time in this regime, the slowest possible spin-down is required. Any faster spin-down only would remove sources from this frequency band without adding more new ones from higher frequencies. Since the slowest possible spin-down without weakening the gravitational-wave signal is attained by switching off dipolar emission, the results from Fig. 5 are a strict upper limit on the gravitational-wave amplitude for $f > 250$ Hz.

To formulate rigorous proof of this claim, we characterize the generalized spin-down such a "mixed" neutron star will experience with a spin-down parameter $\hat{y}$. The spin-down from electromagnetic dipolar emission in terms of the rotation frequency $\nu$ is given by

$$\dot{\nu}_{\mathrm{dip}} = -\frac{2\pi^2}{3c^3}\frac{B_{\mathrm{p}}^2 R^6 \sin^2(\alpha)}{I}\nu^3 =: \gamma_{\mathrm{dip}}\nu^3, \tag{5.1}$$

where $B_{\mathrm{p}}$ is the magnetic field strength at the neutron star's magnetic pole, $\alpha$ is the angle between the rotation axis and the magnetic field, and $R$ is the radius of the neutron star. Rewriting Eq. (2.1) the spin-down from gravitational waves is

$$\dot{\nu}_{\mathrm{gw}} = -\frac{512\pi^4 G}{5c^5} I\varepsilon^2\nu^5 =: \gamma_{\mathrm{gw}}\nu^5. \tag{5.2}$$

A neutron star emitting energy by both mechanisms at once will experience a total spin-down

$$\dot{\nu} = \gamma_{\mathrm{gw}}\nu^5 + \gamma_{\mathrm{dip}}\nu^3. \tag{5.3}$$

This differential equation cannot [in contrast to (2.1)] be solved analytically for $\nu(t)$, yet it can be integrated to give the time $t(\nu, \nu_0)$ in which a neutron star spins down from rotation frequency $\nu_0$ to $\nu$:

$$t(\nu, \nu_0) = \frac{1}{2|\gamma_{\mathrm{dip}}|}\left[\frac{\nu_0^2 - \nu^2}{\nu_0^2\nu^2} + \hat{y}\ln\left(\frac{\nu^2}{\nu_0^2}\left(\frac{1+\hat{y}\nu_0^2}{1+\hat{y}\nu^2}\right)\right)\right], \tag{5.4}$$

where $\hat{y} := \gamma_{\mathrm{gw}}/\gamma_{\mathrm{dip}}$ is the *general spin-down parameter*. Note, that $\hat{y} \to 0$ corresponds to switching off gravitational-wave emission, while $\hat{y} \to \infty$ leads to pure gravitational-wave spin-down. Taking these limits in (5.4), one easily recovers the equations for pure dipolar and gravitational-wave spin-down, respectively, which can be solved analytically for $\nu(t)$.

Let us now turn to the derivation of the expected maximum gravitational-wave amplitude from such neutron stars. The derivation given in Sec. II B is straightforwardly modified to incorporate the generalized spin-down. The generalization of the present-time gravitational-wave frequency distribution $\varrho_f$ is obtained by writing Eq. (2.13) for fixed $t$ and $\hat{y}$ as

$$\varrho_f(f, t, \hat{y})\mathrm{d}f = \varrho_{f_0}(f_0(f, t, \hat{y}))\frac{\partial f_0(f, t, \hat{y})}{\partial f}\mathrm{d}f. \tag{5.5}$$

Note, that (5.4) cannot be solved analytically for $f_0(f, t, \hat{y}) = 2\nu_0(f, t, \hat{y})$. Care has to be taken to evaluate the partial derivative. Taking the total derivative of $t(\nu, \nu_0) = \mathrm{const}$ with respect to $\nu$ and application of the chain rule yields by a straightforward calculation

$$\frac{\partial f_0}{\partial f} = \frac{\partial \nu_0}{\partial \nu} = -\frac{\partial t}{\partial \nu}\cdot\left(\frac{\partial t}{\partial \nu_0}\right)^{-1}. \tag{5.6}$$

Evaluation of this expression by use of (5.4) finally leads to

$$\frac{\partial f_0}{\partial f} = \frac{f_0^3(4 + \hat{y}f_0^2)}{f^3(4 + \hat{y}f^2)}. \tag{5.7}$$

It is easy to see that $\hat{y} \to \infty$ implies $\frac{\partial f_0}{\partial f} \to \frac{f_0^5}{f^5}$, reproducing Eq. (2.15).

However, there is no conceptual difference between a spin-down governed by $\varepsilon$ and one governed by $\hat{y}$. One can write Eq. (2.18) giving the number of neutron stars with fixed spin-down parameter $\hat{y}$ in a frequency band $[f_1, f_2]$ and gravitational-wave amplitude $h \geq h_{\mathrm{max}}$ as

$$M(f_1, f_2, h_{\mathrm{max}}, \hat{y}) = \int_0^{\bar{t}} \mathrm{d}t\dot{n}(t)\int_{f_1}^{f_2}\mathrm{d}f\varrho_f(f, t, \hat{y}) \times \int_{h_{\mathrm{max}}}^{\infty}\mathrm{d}h\varrho_r(r(h), t)\frac{\mathrm{d}r(h)}{\mathrm{d}h}. \tag{5.8}$$

The fact that $h_{\mathrm{max}}$ for given $\hat{y}$, $f_1$, $f_2$ and $M$ is an upper limit on the gravitational-wave amplitude from a population of neutron stars, whose spin-down is governed by $\hat{y}$, can be rephrased as follows: $h_{\mathrm{max}}$ is an upper limit, if $M(f_1, f_2, h_{\mathrm{max}}, \hat{y})$ is maximal as a function of $\hat{y}$. If $M$ is not maximal as a function of $\hat{y}$, then a larger value of $h_{\mathrm{max}}$ in the same frequency band could be found for a different value of $\hat{y}$ giving the same $M$. Thus, it is necessary to identify maxima of $M(f_1, f_2, h_{\mathrm{max}}, \hat{y})$ in $\hat{y}$. These satisfy

$$\frac{\mathrm{d}}{\mathrm{d}\hat{y}}M(f_1, f_2, h_{\mathrm{max}}, \hat{y}) = 0. \tag{5.9}$$

From Eq. (5.8), it is clear that the only term affected by the derivative is $\varrho_f(f, t, \hat{y})$. Applying the chain rule to (5.5) after inserting (5.7) one obtains

$$\frac{\mathrm{d}}{\mathrm{d}\hat{y}}\varrho_f = \frac{\partial \varrho_{f_0}}{\partial f_0}\cdot\frac{\partial f_0}{\partial \hat{y}}\cdot\frac{f_0^3(4 + \hat{y}f_0^2)}{f^3(4 + \hat{y}f^2)} + \varrho_{f_0}\cdot\frac{f_0^3(f_0^2 - f^2)}{f^3(4 + \hat{y}f^2)^2}, \tag{5.10}$$

where the arguments of the functions are suppressed.

Let us show that the last equation implies that the maximum expected amplitude as given in Sec. V B is a rigorous upper limit for frequencies $f_0$ for which

$$\frac{\partial \varrho_{f_0}}{\partial_{f_0}}\Bigg|_{f_0(f,t,\hat{y})} \leq 0 \forall f, t. \tag{5.11}$$

The second summand on the right-hand side of (5.10) is positive $\forall f$, $t$, $\hat{y}$. The last factor in the first summand is always positive. It is also clear, that $\partial_{\hat{y}} f_0 < 0 \forall f$, $t$ for a fixed value of $\varepsilon$ [15]. Therefore, if (5.11) holds true, it follows $\frac{\mathrm{d}}{\mathrm{d}\hat{y}} \varrho_f > 0 \forall f$, $t$, $\hat{y}$, and $\frac{\mathrm{d}}{\mathrm{d}\hat{y}} M > 0 \forall \hat{y}$. Thus, if (5.11) is fulfilled, the global maximum of $M$ as a function of $\hat{y}$ is reached for $\hat{y} \rightarrow \infty$, that is for pure gravitational-wave spin-down.

As mentioned earlier, for the model distribution of initial frequencies adopted to produce Fig. 5 has its maximum at $f_0 = 250$ Hz and is monotonically decreasing for larger values of initial frequencies. Therefore, Eq. (5.11) is fulfilled for $f \geq 250$ Hz in Fig. 5, and the graphs shown there are a strict upper limit on the gravitational-wave amplitude from neutron stars spinning down by gravitational waves and electromagnetic dipolar emission for $f > 250$ Hz.

## VI. CONCLUSIONS

We have used analytical arguments and the results of a numerical simulation to show that the assumptions of Blandford's argument do not hold in a realistic model of our galaxy.

The assumptions (both in the original and in revised formulations of the argument) cannot be fulfilled for realistic values of ellipticity. The spatial scaling dimension $D$ of an evolved neutron star distribution fulfills $D > 2$ making a simple two-dimensional model invalid. The distribution in frequency will not be in a steady state at the present time for realistic values of ellipticity.

Because these two assumptions do not hold, the simple geometrical reasoning behind Blandford's argument is not valid. The numerical simulations provide an improved estimate of the expected maximum amplitude of gravitational waves from gravitars. We also showed that for frequencies $f > 250$ Hz this maximum amplitude is an upper limit for gravitational waves from neutron stars that spin down by gravitational waves and electromagnetic dipole emission.

Although the expected maximum amplitude is lower by about 1 order of magnitude compared to the previous estimates, we would like to stress that in all of the models so far the influence of the Gould belt has been neglected. This young star-forming region (age $\sim$40 Myrs) near the Sun is characterized by an abundance of massive $O$- and $B$-type stars enriching the solar neighborhood with young neutron stars. If there exists a population of gravitars born in the Gould belt, their gravitational-wave signals are more likely to be the first ones to be detected.

## ACKNOWLEDGMENTS

We thank Cristiano Palomba for useful discussions and for helping to compare the results of his numerical simulations with our own work, and Curt Cutler for helpful discussions and calling our attention to the nice upper-limit argument given in Ref. [2]. We also thank the referee for some suggested rewording and clarification of the status of the gravitar existence arguments. B. K. thanks the IMPRS on Gravitational Wave Astronomy for its support. This work was supported in part by DFG Grant SFB/Transregio 7 "Gravitational Wave Astronomy."

[1] K. S. Thorne, in *Three Hundred Years of Gravitation* (Cambridge University Press, Cambridge, England, 1987).
[2] B. Abbott *et al.* Phys. Rev. D **76**, 082001 (2007).
[3] C. Palomba, Mon. Not. R. Astron. Soc. **359**, 1150 (2005).
[4] S. B. Popov, M. Colpi, A. Treves, R. Turolla, V. M. Lipunov, and M. E. Prokhorov, http://de.arXiv.org/abs/astro-ph/9910114.
[5] Detector and Sun can be assumed collocated on galactic scale.
[6] This assumes that the Sun is farther from the edge of the disk than the closest expected source. Since the expected loudest sources are very close to the Sun, this assumption is justified.
[7] $R = 10$ kpc, $\tau_B = 30$ yrs, $I = 10^{38}$ kg m$^2$.
[8] G. Hobbs, D. R. Lorimer, A. G. Lyne, and M. Kramer, Mon. Not. R. Astron. Soc. **360**, 974 (2005).
[9] B. Paczynski, Astrophys. J. **348**, 485 (1990).
[10] I. Yusifov and I. Kucuk, Astron. Astrophys. **422**, 545 (2004).
[11] Z. Arzoumanian, D. F. Chernoff, and J. M. Cordes, Astrophys. J. **568**, 289 (2002).
[12] W. H. Press, B. P. Flannery, S. A. Teukolsky, and W. T. Vetterling, *Numerical Recipes: The Art of Scientific Computing* (Cambridge University Press, Cambridge, England, 1992), 2nd ed..
[13] GSL GNU Scientific Library, URL http://www.gnu.org/software/gsl/.
[14] E.g. a gravitar with $f = 2$ kHz, $\varepsilon = 10^{-6}$ must be as close as $r = 1$ kpc.
[15] Increasing $\hat{y}$ for fixed $\varepsilon$ and therefore fixed $\gamma_{gw}$ is only possible by decreasing $\gamma_{dip}$, that is reducing the amount of energy radiated away by dipolar spin-down. Accordingly, the total spin-down is slower and $f_0$ less.